Journal of Southeast University (English Edition) Vol. 38, No. 4, pp. 350 - 362 Dec. 2022 ISSN 1003—7985

Multiobjective scheduling optimization of bearing production workshop for green manufacturing

Wang Yansen[1] Feng Lijie[2,4] Wang Jinfeng[2,4] Liu Peng[3,4] Zhao Huadong[1]

([1]School of Mechanical and Power Engineering, Zhengzhou University, Zhengzhou 450001, China)
([2]China Institute of FTZ Supply Chain, Shanghai Maritime University, Shanghai 201306, China)
([3]School of Management, Zhengzhou University, Zhengzhou 450001, China)
([4]Henan Engineering Research Center of Innovation Method, Zhengzhou 450001, China)

Abstract: Aiming at the machining process of high-performance bearing parts, the green shop scheduling problem of bearing parts processing was studied herein, with the maximum completion time, minimum machine carbon emission, and minimum grinding fluid usage as the optimization objectives. The manufacturing process is divided into six technological processes: startup, clamping, machining, unloading, standby, and shutdown. The multiobjective green shop scheduling mathematical model is established. Then, an improved multiobjective genetic algorithm is proposed, adopting a segmented coding method that integrates the process and machine selections and improves the steps of crossover and mutation, all of which improve the algorithm's convergence. Finally, the bearing parts processing of a bearing company is taken as a case study, and large-scale data tests and analyses are constructed. The result shows that the proposed model can obtain lower completion time, carbon emission, and grinding fluid consumption, which verifies the scientificity and effectiveness of the proposed model.

Key words: green shop scheduling problem (GSSP); multiobjective optimization; carbon emissions; rolling bearing
DOI: 10.3969/j.issn.1003-7985.2022.04.004

In recent years, in the context of upgrading the manufacturing industry, the application field of green manufacturing has expanded in many fields. As one of the important parts of green manufacturing, green shop scheduling has broad development prospects[1-2]. As one of the core components of complex mechanical products, the processing process of high-performance bearing has the characteristics of a long time and high energy consumption. Unreasonable production planning causes problems, such as high costs and environmental pollution[3]. Therefore, the research on the green shop scheduling problem (GSSP) of high-performance bearing parts processing is greatly important for energy-saving and efficient green manufacturing.

The GSSP has been widely studied by scholars in many fields since it was proposed[4]. Unlike traditional scheduling problems, the GSSP emphasizes the impact of the manufacturing process on the environment and resource efficiency. The complexity of the problem is higher, and the solution is more difficult[5-6]. Several studies have been conducted on this problem. Tian et al.[7] proposed a combination of timed transition Petri net and ant colony optimization algorithm to solve the energy-saving FJSP problem in a manufacturing environment. Yüksel et al.[8] took the minimizing of total delay and energy consumption as objective functions to study the wait-free permutation flow shop scheduling problem and achieved good results in practical cases. Lei et al.[9] designed an improved leapfrog algorithm to solve the low-carbon FJSP problem under multiobjective optimization and achieved good results. Zheng et al.[10] proposed a new multiobjective Drosophila algorithm to solve the unrelated parallel online green workshop scheduling problem. Deng et al.[11] studied the no-wait job-shop scheduling problem and constructed the total flow time criterion of the no-wait job-shop problem based on the time difference. Sang et al.[12] proposed an SV-MA memetic algorithm to solve the high-dimensional multiobjective green flexible job-shop scheduling problem (Ma-OFJSSP). According to the actual manufacturing situation, Gong et al.[13] considered the machine factors and the flexibility of operators and constructed a dual resource mathematical scheduling model. Ic et al.[14] established the mathematical relationship between the surface quality, carbon emission, and cutting parameters in the turning process, and optimized it using the objective programming method. Li et al.[15] constructed a carbon emission function generated when the machine was started, processed, and idle according to the running state of the machine in the processing process.

Received 2022-05-10, **Revised** 2022-10-10.

Biographies: Wang Yansen (1996—), male, Ph. D. candidate; Feng Lijie (1966—), male, doctor, professor, ljfeng@shmtu.edu.cn.

Foundation items: Innovation Method Fund of China (No. 2019IM020200), Joint Funds of the National Natural Science Foundation of China (No. U1904210-4), Zhengzhou University Support Program Project for Young Talents and Enterprise Cooperative Innovation Team, "Intelligent Manufacturing Comprehensive Standardization and New Model Application Project" of Ministry of Industry and Information Technology (No. 2017ZNZX02), Shanghai Science and Technology Program (No. 20040501300).

Citation: Wang Yansen, Feng Lijie, Wang Jinfeng, et al. Multiobjective scheduling optimization of bearing production workshop for green manufacturing[J]. Journal of Southeast University (English Edition), 2022, 38(4): 350 - 362. DOI: 10.3969/j.issn.1003-7985.2022.04.004.

They also solved the low-carbon flexible workshop scheduling problem under multiobjective conditions. Zhang et al.[16] studied the flexible flow shop scheduling problem in the TOU environment. The workshop electricity cost was described in detail. Zhang et al.[17] established a multiobjective integrated scheduling model from the game theory perspective to study the real-time and flexible multiobjective scheduling problem.

Hence, previous studies have established corresponding mathematical models and calculation methods of various green indicators, such as water consumption, power consumption, and carbon emission. However, the research on the deep-seated green indicator system, such as raw material loss and gas emission in the manufacturing process, is relatively lacking. Therefore, the results obtained cannot reflect the green optimization concept for the manufacturing shop floor. Additionally, under the trend of intelligent and integrated development of manufacturing systems, the optimal modeling of raw material loss, gas emission, and other factors in the complex manufacturing process is an important part of green shop scheduling, all of which have become one of the current research hot spots.

Given the above shortcomings, based on the machining process of high-performance bearing parts, taking the maximum completion time, machining process carbon emission, and grinding fluid consumption as the objective functions, this study investigates the multiobjective green job-shop scheduling problem for machining high-performance bearing parts. By comparing the integrated optimization results with the single-objective optimization results considering the maximum completion time, carbon emission, and grinding fluid consumption to verify the advantages of the proposed integrated optimization model in solving such problems.

1 Problem Analysis and Mathematical Modeling

1.1 Problem analysis

The problem can be expressed as follows: there are n workpieces to be processed, the workshop has m machines, and each workpiece has q_i processes. The workpiece process, the optional processing machine, and the corresponding processing time are known. In order to complete the processing tasks of all workpieces, with the completion time, the total carbon emission and total grinding fluid consumption as objective functions, the machining sequence and machine selection of each workpiece are scientifically decided.

The assumptions are as follows:

1) No priority constraint is between different workpieces, but each workpiece must be machined according to the process constraints.

2) The process parameters and machine parameters are known.

3) Only a machine can be selected to process a workpiece at a time, and it is not allowed to be interrupted once it starts.

4) All workpieces and machines are ready at time $t = 0$; the nonprocessing time of the job, such as preparation and transportation times, is ignored. The machine is available during the whole production process.

5) The buffer zone between each processing stage of the job is infinite.

6) The processing machine is only turned on and off once in the process, which means the carbon emission generated by the starting and stopping of the machine tool is fixed.

7) The total load of all machining is within a reasonable range.

1.2 Optimization model of green shop scheduling

1.2.1 Total carbon emission function of machine processing

Due to the high machining accuracy and cumbersome process of high-performance bearing parts, after the process analysis, the total time was divided into six sections: the machine start, fixture installation, workpiece cutting, fixture disassembly, machine standby, and machine shutdown time. Thus, the corresponding machine to produce carbon emissions is divided into six parts: carbon emission of the machine starting once, fixture installation carbon emission, workpiece cutting carbon emission, fixture disassembly carbon emission, machine standby carbon emission, and machine shutdown carbon emission. Additionally, since the machine is cooled by a coolant, the carbon emissions from the machine's coolant use need to be considered. The machine state-energy consumption curve is shown in Fig. 1. The main process is divided into starting, fixture installation, workpiece cutting, fixture disassembly, idling, and shutdown, corresponding to six-time processes, respectively. Herein, the fixture installation, disassembly and job processing power are classified into a category for mathematical modeling and quantitative calculations. The machine startup and shutdown are classified into a category for mathematical modeling and quantitative calculations. The specific modeling process is shown as follows.

Carbon emissions from the machine startup are calculated as follows:

$$E_{\mathrm{st}} = \sum_{k=1}^{m} \sum_{i=1}^{n} \sum_{j=1}^{q_i} (e_{\mathrm{st}} t_{\mathrm{st}}(X_{ijk}) F_{\mathrm{e}}) \tag{1}$$

where E_{st} is the carbon emission from the machine startup; e_{st} is the power at machine startup; t_{st} is the machine startup time; X_{ijk} is the process decision variable. $X_{ijk} = 1$ if O_{ij} is selected to be processed by machine k; otherwise, $X_{ijk} = 0$. O_{ij} is the j-th operation of workpiece i. F_{e} is the carbon emission factor of electrical energy.

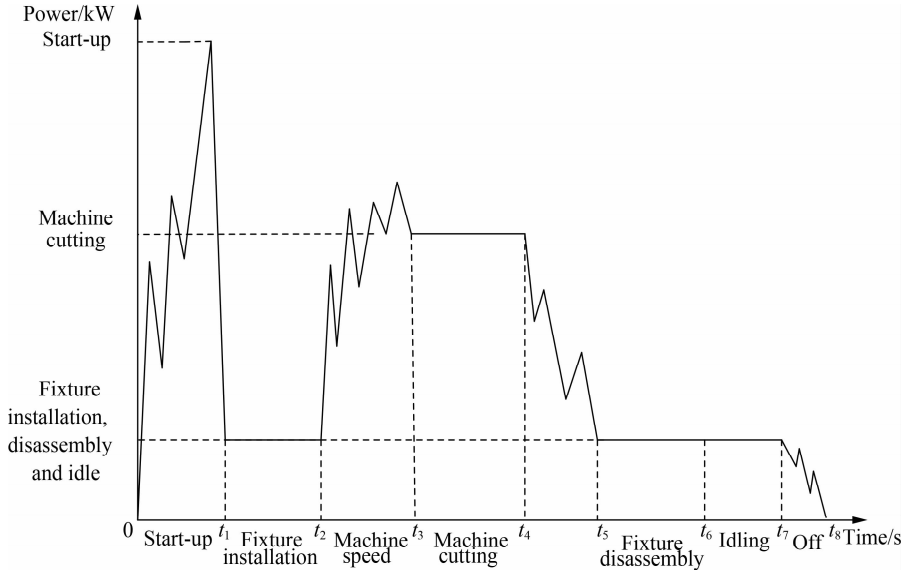

Fig. 1 State-energy consumption distribution curve of machining equipment

The carbon emissions of fixture installation are calculated as follows:

$$E_{\text{ins}} = \sum_{k=1}^{m}\sum_{i=1}^{n}\sum_{j=1}^{q_i}(e_{\text{ins}}t_{\text{ins}}(X_{ijk})F_{\text{e}}) \tag{2}$$

where E_{ins} is the carbon emission of the fixture installation; e_{ins} is the power during the machine tool clamping; and t_{ins} is the machine tool clamping time.

The carbon emissions from the workpiece cutting are calculated as follows:

$$E_{\text{wk}} = \sum_{k=1}^{m}\sum_{i=1}^{n}\sum_{j=1}^{q_i}(e_{\text{wk}}t_{\text{wk}}(X_{ijk})F_{\text{e}}) \tag{3}$$

where E_{wk} is the carbon emission from the workpiece cutting; e_{wk} is the power during the machine processing; and t_{wk} is the processing time of machine k.

The carbon emissions from the fixture disassembly are calculated as follows:

$$E_{\text{uins}} = \sum_{k=1}^{m}\sum_{i=1}^{n}\sum_{j=1}^{q_i}(e_{\text{uins}}t_{\text{uins}}(X_{ijk})F_{\text{e}}) \tag{4}$$

where E_{uins} is the carbon emission from fixture disassembly; e_{uins} is the power when the machine tool is unclamped; and t_{uins} is the machine tool unclamping time.

The standby carbon emissions are calculated as follows:

$$E_{\text{id}} = e_{\text{id}}(S_{i,j,k} - F_{i-1,j,k})F_{\text{e}} \tag{5}$$

where E_{id} is the standby carbon emission; e_{id} is the power when the machine is on standby; $S_{i,j,k}$ is machine k's start time of operation O_{ij}; and $F_{i,j,k}$ is the time for machine k to complete operation O_{ij}.

The carbon emissions from the machine shutdown are calculated as

$$E_{\text{cls}} = \sum_{k=1}^{m}\sum_{i=1}^{n}\sum_{j=1}^{q_i}(e_{\text{cls}}t_{\text{cls}}(X_{ijk})F_{\text{e}}) \tag{6}$$

where E_{cls} is the carbon emissions from machine shutdown; e_{cls} is the machine shutdown power; and t_{cls} is the machine shutdown time.

The carbon emissions from using a coolant are calculated as follows:

$$E_{\text{coo}} = \sum_{k=1}^{m}\sum_{i=1}^{n}\sum_{j=1}^{q_i}\left(\frac{t_{\text{wk}}}{T_{\text{e}}}N_{\text{f}}(X_{ijk})F_{\text{w}}\right) \tag{7}$$

where E_{coo} is the carbon emission from using a coolant; F_{w} is the carbon emission factor of the coolant; T_{e} is the coolant cycle usage; and N_{f} is the cycle usage of the coolant on machine k.

To sum up, the total carbon emissions of machine processing are calculated as

$$E_{\text{mac}} = E_{\text{st}} + E_{\text{ins}} + E_{\text{wk}} + E_{\text{unis}} + E_{\text{id}} + E_{\text{cls}} + E_{\text{coo}} \tag{8}$$

where E_{mac} is the total carbon emissions from machine processing.

1.2.2 Function of total grinding fluid usage in machine processing

The grinding fluid used in the workshop is mainly generated during machine processing. Besides, the amount of grinding fluid used per unit of time varies due to factors such as different machine equipment power and load rate. Herein, the amount of grinding fluid used is calculated according to the use cycle, machine model, and processing time.

The amount of grinding fluid used in machine processing is calculated as follows:

$$W_{\text{e}} = \sum_{k=1}^{m}\sum_{i=1}^{n}\sum_{j=1}^{q_i}\left(\frac{t_{\text{wk}}}{T_{\text{h}}}N_{\text{h}}(X_{ijk})M_k\right) \tag{9}$$

where W_e is the total amount of grinding fluid used in machine processing; t_{wk} is the processing time of operation O_{ij} on machine k; T_h is the use cycle of the grinding fluid; N_h is the cycle usage of the grinding fluid on machine k; and M_k is the selected machine number.

1.2.3 Model establishment and constraints

Based on the above analysis, an integrated scheduling mathematical model and constraints are constructed based on the objective functions of the maximum completion time, minimizing total carbon emissions from machine processing, and minimizing total grinding fluid usage in machine processing.

$$\text{Min}Z = T_i + E_{mac} + W_e \tag{10}$$

The maximum completion time is calculated as follows:

$$T_i = \min[\max(T_i)] \tag{11}$$

The total carbon emissions from machine processing are calculated as follows:

$$E_{mac} = \min(E_{mac}) \tag{12}$$

The total amount of grinding fluid used in machine processing is calculated as follows:

$$W_e = \min(W_e) \tag{13}$$

s. t.

$$\sum_{k=1}^{M} X_{ijk} = 1 \tag{14}$$

$$[S_{i,j,k} - (S_{i,(j-1),k} + t_{i,(j-1),k})]X_{ijk} \geqslant 0 \tag{15}$$

$$S_{(i+1),j,k} - F_{i,j,k} \geqslant 0 \tag{16}$$

$$T_i \leqslant T_{i0};\ E_{mac} \leqslant E_{mac0};\ W_e \leqslant W_{e0} \tag{17}$$

where T_i is the maximum completion time; E_{mac} is the total carbon emission of machine processing; W_e is the total amount of grinding fluid used during machining; T_{i0} is the maximum completion time constraint; E_{mac0} is the carbon emission constraint; and W_{e0} is the grinding fluid usage constraint.

The objective function Eq. (10) comprises three parts, namely Eqs. (11) to (13). In Eq. (10), T_i represents the completion time, E_{mac} represents the total carbon emission of machine processing, and W_e represents the total amount of the grinding fluid used during machining. In the constraint conditions, Eq. (14) indicates that any procedure can select only one piece of equipment for processing. Eq. (15) indicates that the job must meet the process order constraints of the workpiece. Eq. (16) indicates that each processing machine can only process a workpiece at a time. Eq. (17) expresses the objective function constraint; T_{i0} represents the maximum completion time constraint, E_{mac0} represents the carbon emission constraint, and W_{e0} represents the grinding fluid usage constraint; that is, the processing of each job must be conducted under the premise of guaranteeing the actual production status.

2 Proposed Algorithm

Since its proposal, the multiobjective genetic algorithm (NSGA-Ⅱ) has been widely used in job-shop scheduling problems[18-19]. For the GSSP of bearing parts herein, first, the process arrangement of bearing parts processing is solved. Next, reasonable processing machines are arranged for each process. Based on the non-dominated sorting genetic algorithm, this study proposed an improved solution strategy, which is improved in the steps of crossover and mutation to avoid premature convergence and achieved good solution results. Finally, a set of Pareto frontier scheduling schemes is obtained.

2.1 Two-step coding scheme based on process-machine matching

Herein, a set of coding schemes is randomly generated according to the processing limits and optional machines of bearing parts. First, the process arrangement problem is solved. All parts are processed according to rough grinding, outer diameter, groove, inner diameter, and super-finishing order. The process of each workpiece is represented by 1, 2, and 3. Then, according to each process, the processing machine is selected to solve the machine selection problem, which in turn represents the processing machine serial number of each process selection of the job. This coding method can satisfy both the constraint relation of the machining procedure and the flexible constraint of the machine. The processing information of bearing parts is presented in Tab. 1.

2.1.1 Two-step coding scheme based on process-machine matching

According to the processing procedure and optional machine of the bearing parts, a two-step coding scheme for the process-machine matching is generated. The specific steps are as follows:

1) The five processing procedures of bearings: rough grinding, outer diameter, groove, inner diameter, and super-finishing are coded to obtain the sequence code of the bearing processing technology, which is denoted as $\{N_{x1}, N_{x2}, \cdots, N_{x5}\}$.

2) The code for the machine with the roughing is selected. The roughing procedure is selected from the bearing working procedure sequence, and the machine sequence is arranged and coded symbolically, denoted as $\{N_{x1} \mid M_{11}, M_{12}, \cdots, M_{1\alpha}\}$, where α represents the number of optional machines for rough grinding. Second, the code for the machine with the outer diameter is selected. The outer diameter procedure is selected from the bearing working procedure sequence, and the machine sequence is

Tab. 1 Processing information sheet

Workpiece	Work sequence	Craft name	Process time/s							
			M_1	M_2	M_3	M_4	M_5	M_6	M_7	M_8
J_1	N_{11}	Rough grinding	55							
	N_{12}	Outer diameter		56	57					
	N_{13}	Groove				56	58			
	N_{14}	Inner diameter						60	57	
	N_{15}	Super-finishing								55
J_2	N_{21}	Rough grinding	56							
	N_{22}	Outer diameter		58	57					
	N_{23}	Groove				58	59			
	N_{24}	Inner diameter						59	58	
	N_{25}	Super-finishing								56
J_3	N_{31}	Rough grinding	57							
	N_{32}	Outer diameter		58	55					
	N_{33}	Groove				56	58			
	N_{34}	Inner diameter						58	55	
	N_{35}	Super-finishing								58

arranged and coded symbolically, denoted as $\{N_{x2} \mid M_{21}, M_{22}, \cdots, M_{2\beta}\}$, where β represents the number of optional machines for the outer diameter. Next, the code for the machine with the groove is selected. The groove working procedure is selected from the bearing working procedure sequence, and the machine sequence is arranged and coded symbolically, denoted as $\{N_{x3} \mid M_{31}, M_{32}, \cdots, M_{3\gamma}\}$, where γ represents the number of optional machines for groove. Then, the code for the machine with the inner diameter is selected. The inner diameter procedure is selected from the bearing working procedure sequence, and the machine sequence is arranged and coded symbolically, denoted as $\{N_{x4} \mid M_{41}, M_{42}, \cdots, M_{4\delta}\}$, where δ represents the number of optional machines for the inner diameters. Finally, the code for the machine with the super-finishing is selected. The super-finishing procedure is selected from the bearing working procedure sequence, and the machine sequence is arranged and coded symbolically, denoted as $\{N_{x5} \mid M_{51}, M_{52}, \cdots, M_{5\eta}\}$, where η represents the number of optional machines for super-finishing.

2.1.2 Generation of the initial machining scheme set

First, the number of job processing schemes is set as I. Second, the work-oriented process-machine processing sequence is set. Based on the coding sequence of the bearing processing technology: $\{N_{x1}, N_{x2}, N_{x3}, N_{x4}, N_{x5}\}$, the processing procedures are successively selected for the job, and idle machines are selected from the machine configuration coding sequence of the corresponding process to form a process-oriented machine-processing sequence, denoted as $\{J_{11} \mid N_{11} - M_{1\alpha}, N_{12} - M_{2\beta}, \cdots, N_{15} - M_{5\eta}\}$. Next, according to the previous step, the execution is performed b times to generate b process-machine sequences to form the set of the process-machine sequences of the job denoted as $\{J_1 \mid J_{11}, J_{12}, \cdots, J_{1b}\}$. Finally, the initial work-process-machine processing sequence set is generated, and the above steps are repeated for each artifact to obtain a process-machine sequence set for all artifacts, given n artifacts $\{J \mid J_1, J_2, \cdots, J_n\}$.

To explain the above principle, the coding process is detailed in Tab. 1 as an example. In Tab. 1, N_{ij} represents the j-th process of workpiece i. For example, N_{32} represents the second process of job J_3. A blank area indicates ms ($s = 1, 2, \cdots, 5$) cannot process the current process, the same as below. As shown in Tab. 2, J_1, J_2, and J_3 all have five processes, so in the coding scheme [3 1 2 2 2 1 2 3 3 2 1 1 1 2 3 2 4 5 5 6 7 7 8 8 8], the process part [3 1 2 2 1 3 3 2 1 2 1 3 3 2 1 2 1 3 3 2 1 2 1 3 3 1] indicates that the processing sequence of all job processes is $N_{31} \rightarrow N_{11} \rightarrow N_{21} \rightarrow N_{22} \rightarrow N_{12} \rightarrow N_{32} \rightarrow N_{33} \rightarrow N_{23} \rightarrow N_{13} \rightarrow N_{24} \rightarrow N_{14} \rightarrow N_{34} \rightarrow N_{35} \rightarrow N_{25} \rightarrow N_{15}$. Similarly, the equipment part [1 1 1 2 3 2 4 5 5 6 7 7 8 8 8] represents the following. Procedures N_{31}, N_{11}, N_{21}, N_{22}, N_{12}, and N_{32} are processed on M_1, M_1, M_1, M_2, M_3, and M_2, respectively, and the rest are similar. The encoding scheme is shown in Fig. 2.

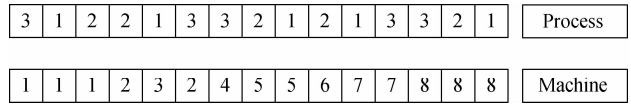

Fig. 2 Chromosomal coding

During decoding, the machine matrix of all processes can be obtained, and the machining time matrix of all processes can be obtained according to the corresponding machining time. Finally, it can be transformed into an effective scheduling scheme. According to the decoding process and the data in the table above, the combination of the work-process-machine processing time of the bearing parts can be obtained as N_{11}-M_1-55, N_{12}-M_3-57, and N_{13}-M_5-58, and the rest are similar.

2.2 Selection

This study adopts the method of tournament selection. According to the niche concept based on the crowding idea, the crowding distance $\varepsilon(i)$ helps to sort all individuals in the noninferior solution set according to the crowding comparison operation[20]. The crowding distance between each individual in the group and two adjacent individuals of the same level is calculated by presetting the level and the repetition value. Afterward, the multiresidual noninferior solutions are deleted to screen outstanding individuals and finally obtain their noninferior solution frontier.

2.3 Crossover

In the process sequence string, the single-point crossover operator cannot guarantee that the workpiece number i in the progeny chromosome has and only appears n_i times, which cannot guarantee the feasibility of the solution. Based on this, this study adopts the hybrid method of the POX crossing and single-point crossing principle to conduct crossover operations. This crossover mode enables the information of the parent chromosome to be retained in the offspring chromosome (see Fig. 3).

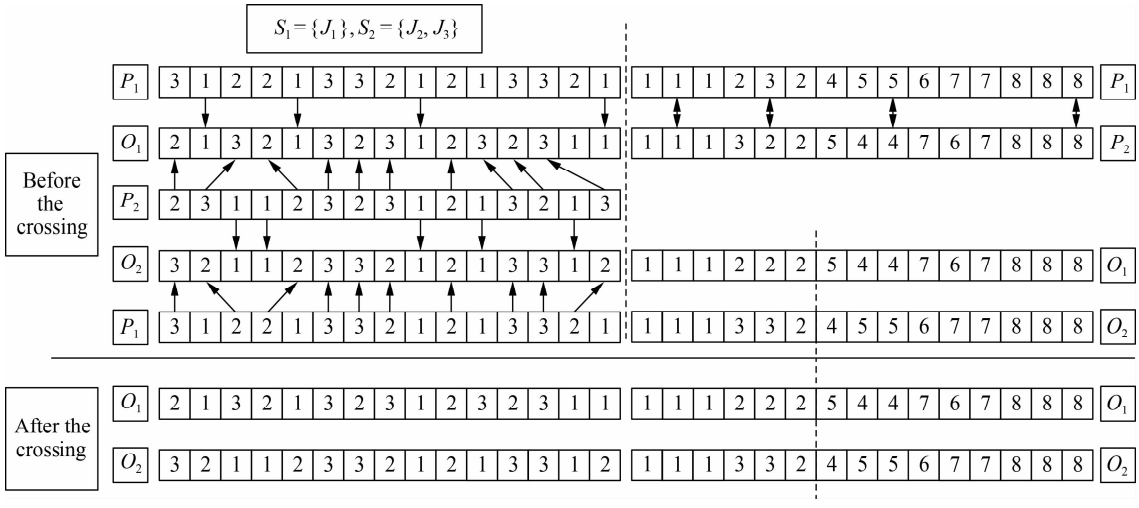

Fig. 3 Crossover operation

The specific steps for the cross-operation of process parts are as follows: first, two chromosomes, P_1 and P_2, are randomly selected, and two empty progeny chromosomes, O_1 and O_2, are initialized. All artifacts, J_1, J_2, and J_3, are randomly divided into two nonempty sets, $S_1 = \{J_1\}$ and $S_2 = \{J_2, J_3\}$. Then, the corresponding genes belonging to the set S_1 in P_1 are copied to the same locus in O_1, and the remaining genes are filled into the vacancy of O_1 in sequence from left to right after deleting the identified genes in O_1 in P_2. Next, the P_1 and P_2 roles are switched, and O_2 is created similarly.

The machine selection part draws on the idea of single-point crossover, and the specific steps are as follows: first, according to the selected two chromosomes, P_1 and P_2, and the generated sets, S_1 and S_2, a set is randomly selected as the crossover point. Next, the machine part of the set is exchanged with each other, whereas the remaining parts remain unchanged to generate two new chromosomes, O_1 and O_2.

2.4 Mutations

Since the alleles of each locus on the chromosome differ in the machine selection substring, the exchange of genes at different loci makes the offspring chromosome unable to be decoded into a feasible scheduling scheme, which cannot guarantee the feasibility of the solution. Based on this, this study uses the concepts of exchange and polynomial mutations for reference to perform mutation operations. First, two parent chromosomes are mutated to obtain two offspring chromosomes so that the information of the parent chromosome can be retained in the offspring chromosome (see Fig. 4). The specific steps

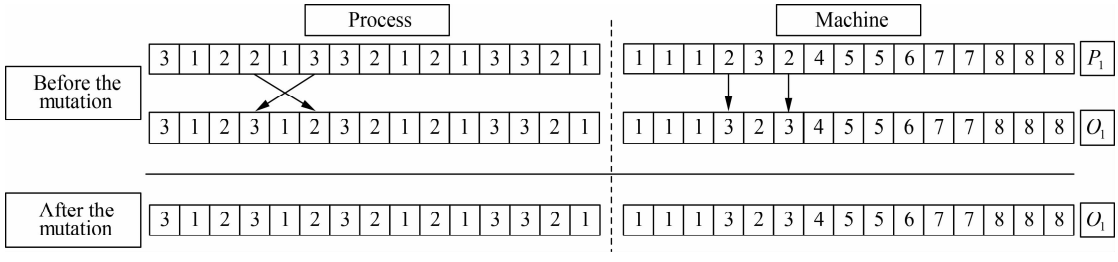

Fig. 4 Mutation operation

are as follows: on the premise of ensuring the process order constraint of the workpiece, two loci are randomly extracted from chromosome P_1. Furthermore, the genes on the two loci are exchanged to produce a new chromosome O_1.

For the parts of the machine, because there is a candidate for every working procedure of the processing machine, the mutation of the machine parts randomly selects a machine set of genes on the period of chromosomes P_1. Then, the corresponding process of the machine is set in the candidate set of machines to select the shortest processing time to replace the machine and reassign the formation of new chromosomes to the original process.

2.5 Optimal scheme set termination rule

This paper adopts the method of setting the maximum number of optimization iterations. First, ω is set as the maximum number of iterations. Next, the iterative optimization is repeated ω times to constantly update the scheduling scheme to obtain the optimal scheme set.

3 Case Study

3.1 Process parameters

The high-performance bearings include an inner ring, outer ring, rolling element, and other parts. The processing process mainly includes rough grinding, fine grinding, and heat treatment. The processing technology of the bearing is complex, involving dozens of specific manufacturing processes. The production process is cumbersome, requiringvarious machinery and equipment, and is usually a mixed processing method of multiple models. To facilitate the research, this study scientifically and reasonably simplifies and adjusts the processing technology, machine parameters, and other information. Taking the P_4 high-performance bearing of a bearing manufacturing enterprise as an example, this study investigates the discrete processing of the inner and outer ring parts of the bearing. The workshop machine parameter information is shown in Tabs. 2 to 4, respectively, given the process composition, optional machines, and processing times of the various bearing parts. Tabs. 5 and 6 give the using information on the coolant and grinding fluid, respectively. Tab. 7 presents the carbon emission factors.

Tab. 2 Machine information sheet

Machine group number	Machine group	Rated power/kW	Idling power/kW	One start/shutdown time/s
M_1	Rough grinding machine set	23	5.0	90/90
M_2, M_3	External grinding machine	23	5.0	90/90
M_4, M_5	Groove grinding machine	23	5.0	90/90
M_6, M_7	Internal grinding machine	23	5.0	90/90
M_8	CNC lathe	23	5.0	90/90
M_9	Rough grinding machine set	36	8.2	90/90
M_{10}, M_{11}	External grinding machine	36	8.2	90/90
M_{12}, M_{13}	Groove grinding machine	36	8.2	90/90
M_{14}, M_{15}	Internal grinding machine	36	8.2	90/90
M_{16}	CNC lathe	36	8.2	90/90

Tab. 3 Bearing inner ring information table

Workpiece	Work sequence	Workpiece process	Fixture installation time/workpiece cutting time/fixture disassembly time/s							
			M_1	M_2	M_3	M_4	M_5	M_6	M_7	M_8
7005 inner ring	O_{11}	Coarse grinding	15/90/10							
	O_{12}	Fine grinding outer diameter		13/80/12	13/84/12					
	O_{13}	Fine grinding channel				15/90/10	15/94/10			
	O_{14}	Fine grinding inner diameter						13/94/12	13/98/12	
	O_{15}	Super-finishing								13/56/12
7006 inner ring	O_{21}	Coarse grinding	15/96/10							
	O_{22}	Fine grinding outer diameter		13/82/12	13/88/12					
	O_{23}	Fine grinding channel				15/90/10	15/94/10			
	O_{24}	Fine grinding inner diameter						13/92/12	13/98/12	
	O_{25}	Super-finishing								13/58/12
7007 inner ring	O_{31}	Coarse grinding	15/105/10							
	O_{32}	Fine grinding outer diameter		13/86/12	13/90/12					
	O_{33}	Fine grinding channel				15/94/10	15/98/10			
	O_{34}	Fine grinding inner diameter						13/94/12	13/100/12	
	O_{35}	Super-finishing								13/60/12
7008 inner ring	O_{41}	Coarse grinding	15/108/10							
	O_{42}	Fine grinding outer diameter		13/94/12	13/96/12					
	O_{43}	Fine grinding channel				15/98/10	15/100/10			
	O_{44}	Fine grinding inner diameter						13/96/12	13/102/12	
	O_{45}	Super-finishing								13/62/12
7009 inner ring	O_{51}	Coarse grinding	15/111/10							
	O_{52}	Fine grinding outer diameter		13/96/12	13/98/12					
	O_{53}	Fine grinding channel				15/94/10	15/100/10			
	O_{54}	Fine grinding inner diameter						13/98/12	13/102/12	
	O_{55}	Super-finishing								13/62/12

Tab. 4 Bearing outer ring information table

Workpiece	Work sequence	Workpiece process	Fixture installation time/workpiece cutting time/fixture disassembly time/s							
			M_9	M_{10}	M_{11}	M_{12}	M_{13}	M_{14}	M_{15}	M_{16}
7005 outer ring	O_{11}	Coarse grinding	15/96/10							
	O_{12}	Fine grinding outer diameter		13/84/12	13/86/12					
	O_{13}	Fine grinding channel				15/96/10	15/100/10			
	O_{14}	Fine grinding inner diameter						13/92/12	13/94/12	
	O_{15}	Super-finishing								15/58/10
7006 outer ring	O_{21}	Coarse grinding	15/99/10							
	O_{22}	Fine grinding outer diameter		13/84/12	13/90/12					
	O_{23}	Fine grinding channel				15/98/10	15/102/10			
	O_{24}	Fine grinding inner diameter						13/94/12	13/96/12	
	O_{25}	Super-finishing								15/60/10
7007 outer ring	O_{31}	Coarse grinding	15/111/10							
	O_{32}	Fine grinding outer diameter		13/90/12	13/92/12					
	O_{33}	Fine grinding channel				15/98/10	15/100/10			
	O_{34}	Fine grinding inner diameter						13/94/12	13/98/12	
	O_{35}	Super-finishing								15/62/10
7008 outer ring	O_{41}	Coarse grinding	15/117/10							
	O_{42}	Fine grinding outer diameter		13/92/12	13/98/12					
	O_{43}	Fine grinding channel				15/100/10	15/102/10			
	O_{44}	Fine grinding inner diameter						13/98/12	13/102/12	
	O_{45}	Super-finishing								15/62/10
7009 outer ring	O_{51}	Coarse grinding	15/120/10							
	O_{52}	Fine grinding outer diameter		13/94/12	13/98/12					
	O_{53}	Fine grinding channel				15/104/10	15/106/10			
	O_{54}	Fine grinding inner diameter						13/104/12	13/108/12	
	O_{55}	Super-finishing								15/66/10

Tab. 5 Coolant usage information sheet

Equipment number	M_1	M_2	M_3	M_4	M_5	M_6	M_7	M_8	M_9	M_{10}	M_{11}	M_{12}	M_{13}	M_{14}	M_{15}	M_{16}
Amount of coolant used/L	30	30	30	30	30	30	30	30	30	30	30	30	30	30	30	30
Use cycle/10^3 s	15	15	24	16	16	18	18	14	14	20	24	16	16	12	12	18

Tab. 6 Grinding fluid usage information sheet

Equipment number	M_1	M_2	M_3	M_4	M_5	M_6	M_7	M_8	M_9	M_{10}	M_{11}	M_{12}	M_{13}	M_{14}	M_{15}	M_{16}
Amount of grinding fluid used/L	9.3	3.6	4.3	4.5	3.8	4.5	4.7	4.3	9.9	3.8	4.3	4.2	3.7	4.7	3.8	4.5
Use cycle/s	60	60	60	60	60	60	60	60	60	60	60	60	60	60	60	60

Tab. 7 Carbon emission factors

Resources	Carbon emission factors
Electricity/(kg · kW^{-1} · h^{-1})	0.674 7
Coolant/(kg · L^{-1})	2.862 0

3.2 Optimization results

According to the given parameter information, the experiment is designed. The initial population is 100, the number of iterations is 100, the crossover operation probability is 0.9, and the mutation operation probability is 0.1. The running results of the algorithm provide a set of Pareto solutions for the production scheduling of the processing of bearing parts. The obtained Pareto-nondominated frontier solutions are shown in Fig. 5. The objective function values are presented in Tab. 8 (20 groups are selected, numbered from top to bottom).

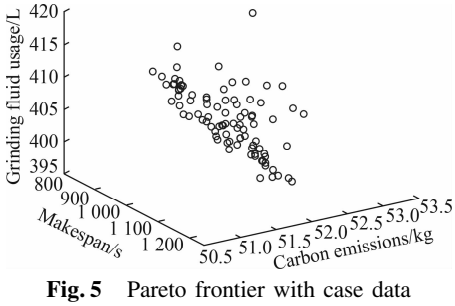

Fig. 5 Pareto frontier with case data

Tab. 8 Pareto frontier solution set

Serial number solution	Completion time/s	Carbon emissions/kg	Grinding fluid usage/L
1	1 111	51.386 6	406.751 7
2	907	52.021 1	405.648 3
3	950	52.060 4	402.508 3
4	899	52.444 2	404.328 3
5	1 006	52.404 4	396.821 7
6	917	51.523 0	409.428 3
7	1 125	52.052 2	399.101 7
8	1 006	51.333 8	407.075 0
9	1 234	50.985 0	410.478 3
10	910	53.370 3	400.171 7
11	975	52.189 2	400.895 0
12	918	51.578 0	407.525 0
13	1 072	52.106 8	400.548 3
14	1 099	51.788 7	402.275 0
15	888	52.752 2	416.611 7
16	1 240	51.466 7	404.235 0
17	974	51.495 5	408.338 3
18	1 006	52.404 4	396.821 7
19	998	52.424 7	398.415 0
20	960	51.157 9	412.481 7

As shown in Tab. 8, when the maximum completion

time is 888 s, the total carbon emission is 52.752 2 kg, and the consumption of the grinding fluid is 416.611 7 L. When the minimum total carbon emission is 50.985 0 kg, the completion time is 1 234 s, and the consumption of the grinding fluid is 410.478 3 L. When the minimum amount of grinding fluid is 396.821 7 L, the maximum completion time is 1006 s, and the carbon emission is 52.404 4 kg. Evidently, three optimization goals conflict with each other. In the actual production environment, it is necessary to select the appropriate scheduling scheme according to different situations. In the Pareto solution set, the Gantt charts of scheduling schemes with maximum completion time (No. 15), minimum carbon emission (No. 10), and minimum grinding fluid use (No. 18) are generated, respectively (see Fig. 6). The Gantt chart includes the processing sequence and machine selection of each workpiece. The numbers represent the corresponding processes of the workpieces. For example, 2-1 represents the processing and time of process 1 for workpiece 2.

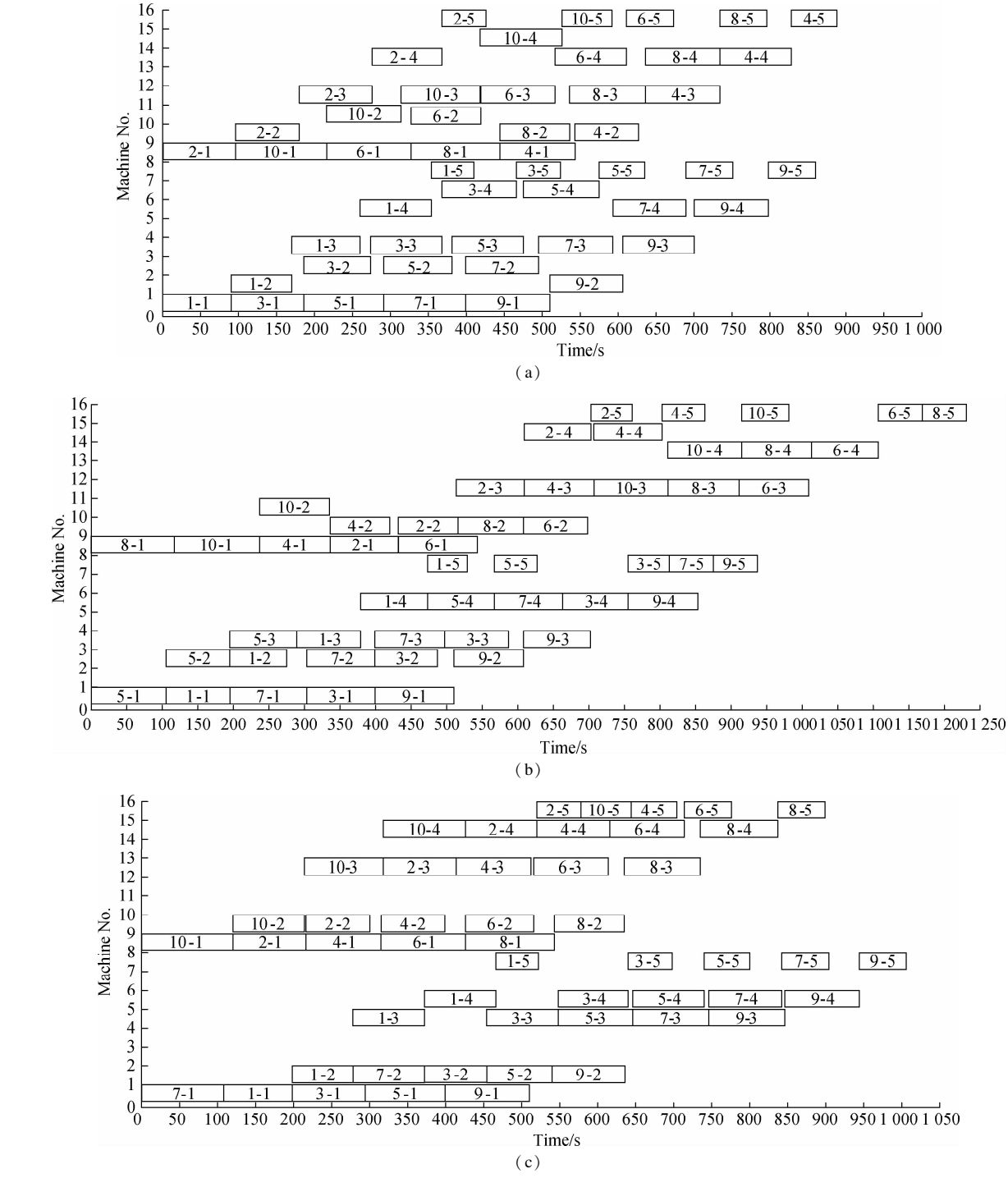

Fig. 6 The Gantt charts of the integrated optimization model. (a) Maximum completion time minimum Gantt chart; (b) Minimum Gantt chart of total carbon emissions; (c) Minimum Gantt chart of grinding fluid usage

3.3 Comparison and verification

To verify the effectiveness of the integrated optimization model, the integrated optimization results are compared with the optimization results of the single-objective model with the maximum completion time, minimum carbon emission, and minimum grinding fluid consumption. When considering the maximum completion time, carbon emission, and grinding fluid consumption separately, the Gantt charts of the optimal single-objective scheme scheduling are shown in Fig. 7, and the resulting pair is presented in Tab. 9.

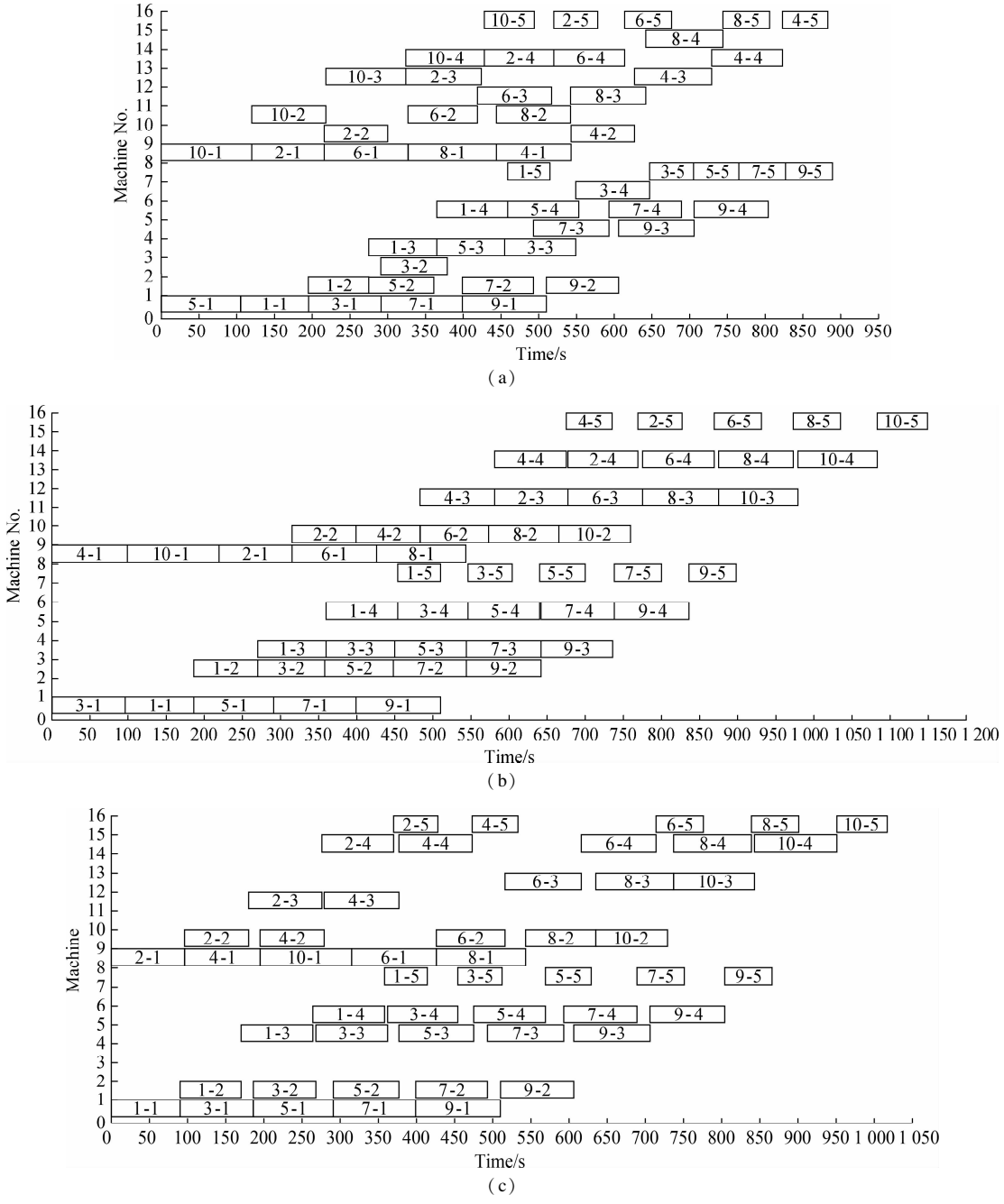

Fig. 7 The Gantt charts of the single objective model. (a) Maximum completion time minimum Gantt chart; (b) Minimum Gantt chart of total carbon emissions; (c) Minimum Gantt chart of grinding fluid usage

Tab. 9 Comparison of optimization results

Model category	Maximum completion time/s	Carbon emissions/kg	Grinding fluid usage/L
Integrated scheduling model	888	52.752 2	416.611 7
	1 234	50.985 0	410.478 3
	1 006	52.404 4	396.821 7
Maximum completion time model	889	52.833 0	410.985 0
Carbon emissions model	1 149	50.779 1	416.878 3
Amount of grinding fluid usage model	1 017	53.137 8	397.945 0

The above chart shows that when the maximum completion time is considered separately, the optimization result is as follows: maximum completion time is 889 s, total carbon emission is 52.833 0 kg, and consumption of grinding fluid is 410.985 0 L. When considering the minimum total carbon emission alone, the optimization result is as follows: maximum completion time is 1 149 s, total carbon emission is 50.779 1 kg, and consumption of grinding fluid is 416.878 3 L. When the minimum amount of grinding fluid is considered separately, the optimization result is as follows: maximum completion time is 1 017 s, total carbon emission is 53.137 8 kg, and amount of grinding fluid is 397.945 0 L. Comparative analysis shows that when a certain objective function is optimized alone, the result cannot make the overall objective optimal. Generally, the single-objective optimization result is worse than that of the multiobjective solution set in the integrated optimization. Therefore, the multiobjective integrated optimization model proposed herein effectively reduces the completion time, carbon emissions, and grinding fluid consumption. In the actual production environment, the appropriate Pareto solution has very strong practicability and can be selected according to the demand, all of which also verify the effectiveness of the proposed model.

3.4 Experiments with different data scales

In bearing manufacturing workshops, different large-scale batch production is often required, so small-scale data experiments have certain limitations and cannot truly reflect the production situation of bearing manufacturing workshops. Therefore, the following conditions were added: the number of bearings of each type was successively set as 5, 10, 20, and 40. For research convenience, the constraint, such as the workshop buffer, is not considered, and the rest information is unchanged. Furthermore, the case analysis of large-scale bearing processing was studied. The Pareto-nondominated front solutions are shown in Fig. 8, and the experimental results are presented in Tab. 10 (three decimal points are kept).

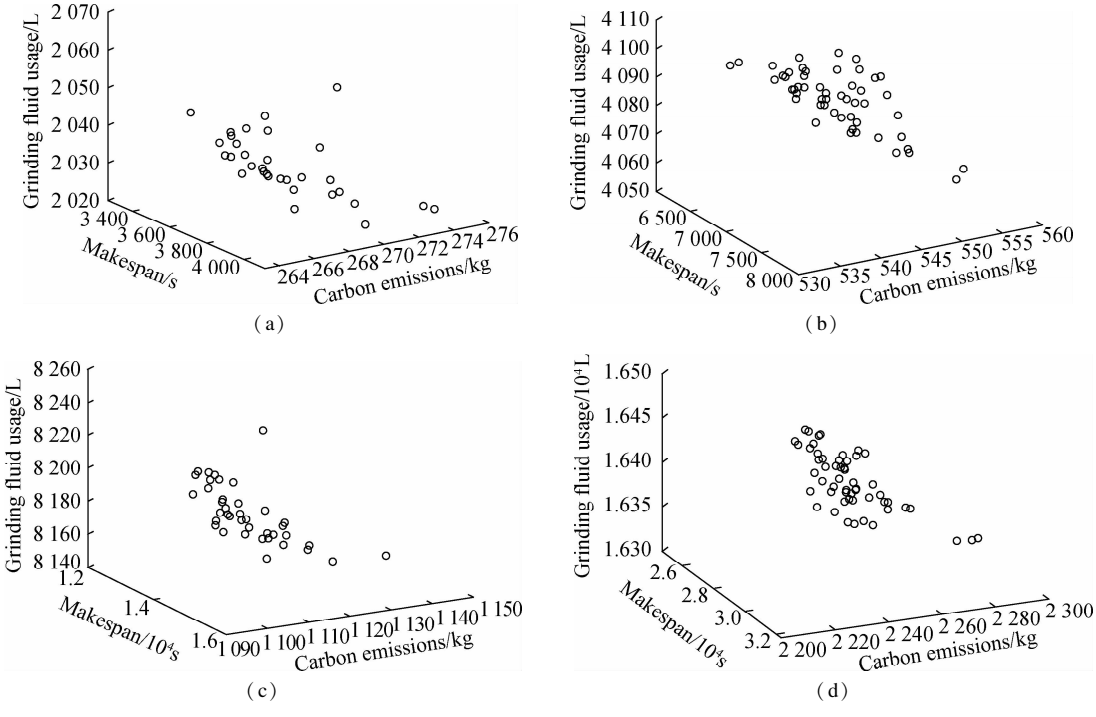

Fig. 8 Pareto frontiers with different data scales. (a) Pareto frontier 5; (b) Pareto frontier 10; (c) Pareto frontier 20; (d) Pareto frontier 40

Evidently, compared with the single-objective scheduling model, the integrated scheduling model proposed herein has a more prominent effect in large-scale data experiments. Furthermore, compared with the single-objective optimization process, the integrated scheduling model results in a more uniform load among the machines, which is more consistent with the actual manufacturing requirements. Therefore, in the actual bearing manufacturing workshop, the multiobjective integrated optimization model can effectively utilize the workshop resources to promote energy saving and emission reduction and realize the green manufacturing process.

4 Conclusions

1) Aiming at the green shop scheduling problem of the processing of high-performance bearing parts, an integrated model is constructed with the maximum completion time and the minimum carbon emission and grinding fluid usage as the objective function by analyzing the process route and parameters of bearing parts.

Tab. 10 Experimental results with different data scales

Model category		Objective function	Number of bearings			
			5	10	20	40
Integrated scheduling model	Completion time	Maximum completion time/s	3 279	6 396	12 601	24 640
		Total carbon emissions/kg	276.458	554.253	1 114.592	2 258.666
		Grinding fluid usage/L	2 037.755	4 082.190	8 189.607	16 404.597
	Carbon emissions	Maximum completion time/s	4 123	6 594	15 520	32 202
		Total carbon emissions/kg	263.325	533.916 0	1 095.733	2 220.073
		Grinding fluid usage/L	2 060.478	4 100.447	8 224.897	16 434.133
	Amount of grinding fluid usage	Maximum completion time/s	3 926	6 775	14 439	28 343
		Total carbon emissions/kg	271.178	552.848	1 141.834	2 296.440
		Grinding fluid usage/L	2 020.002	4 061.823	8 152.383	16 320.790
Maximum completion time model		Maximum completion time/s	3 238	6 205	12 335	24 200
		Total carbon emissions/kg	274.188	547.516	1 125.981	2 196.421
		Grinding fluid usage/L	2 051.958	4 105.097	8 196.563	16 423.763
Carbon emissions model		Maximum completion time/s	3 412	7 105	14 352	26 544
		Total carbon emissions/kg	260.677	525.733	1 055.324	2 144.758
		Grinding fluid usage/L	2 053.315	4 105.943	8 211.13	16 427.3
Amount of grinding fluid using model		Maximum completion time/s	3 948	7 692	14 347	27 158
		Total carbon emissions/kg	277.509	557.715	1 124.339	2 278.693
		Grinding fluid usage/L	2 022.718	4 063.153	8 156.170	16 339.860

2) The solution strategy to solve the problem is proposed, including adopting the segmented coding method, integrating the process and machine selections, and setting improved crossover and mutation operators.

3) The production workshop of a bearing company was taken as a case study. In comparison with the single-objective scheduling model considering the maximum completion time, carbon emission, and grinding fluid consumption separately, the result shows that the proposed model can realize the integrated optimization of the green processing of bearing parts.

4) Due to the limitations of this study, future research will focus on the influence of machine maintenance and material shortage. Besides, the optimization of green indicators, such as noise and toxic substances emissions, will also be considered.

References

[1] Afsar S, Palacios J J, Puente J, et al. Multi-objective enhanced memetic algorithm for green job shop scheduling with uncertain times[J]. *Swarm and Evolutionary Computation*, 2022, **68**: 101016. DOI: 10.1016/j.swevo.2021.101016.

[2] Li H C, Duan J G, Zhang Q L. Multi-objective integrated scheduling optimization of semi-combined marine crankshaft structure production workshop for green manufacturing[J]. *Transactions of the Institute of Measurement and Control*, 2021, **43**(3): 579 - 596. DOI: 10.1177/0142331220945917.

[3] Zong N F, Zhang H, Liu Y, et al. Research and application progress of rolling down technology for continuous casting bearing steel[J]. *Bearing*, 2018(1): 58 - 64. DOI: 10.19533/j.issn1000-3762.2018.01.017. (in Chinese)

[4] Geng K F, Ye C M, Wu S X, et al. Multi-objective green reentrant hybrid flow shop scheduling under tou price[J]. *China Mechanical Engineering*, 2020, **31**(12): 1469 - 1480. DOI: 10.3969/j.issn.1004-132X.2020.12.011. (in Chinese)

[5] Wang L, Wang J J, Wu C G. Advances in green shop scheduling and optimization[J]. *Control and Decision*, 2018, **33**(3): 385 - 391. DOI: 10.13195/j.kzyjc.2017.0215. (in Chinese)

[6] Bekkar A, Belalem G, Beldjilali B. Iterated greedy insertion approaches for the flexible job shop scheduling problem with transportation times constraint[J]. *International Journal of Manufacturing Research*, 2019, **14**(1): 43 - 66. DOI: 10.1504/ijmr.2019.096746.

[7] Tian S L, Wang T Y, Zhang L, et al. An energy-efficient scheduling approach for flexible job shop problem in an internet of manufacturing things environment[J]. *IEEE Access*, 2019, **7**: 62695 - 62704. DOI: 10.1109/ACCESS.2019.2915948.

[8] Yüksel D, Taşgetiren M F, Kandiller L, et al. An energy-efficient bi-objective no-wait permutation flowshop scheduling problem to minimize total tardiness and total energy consumption[J]. *Computers & Industrial Engineering*, 2020, **145**: 106431. DOI: 10.1016/j.cie.2020.106431.

[9] Lei D M, Zheng Y L, Guo X P. A shuffled frog-leaping algorithm for flexible job shop scheduling with the consideration of energy consumption[J]. *International Journal of Production Research*, 2017, **55**(11): 3126 - 3140. DOI: 10.1080/00207543.2016.1262082.

[10] Zheng X L, Wang L. A collaborative multiobjective fruit fly optimization algorithm for the resource constrained unrelated parallel machine green scheduling problem[J]. *IEEE Transactions on Systems, Man, and Cybernetics: Systems*, 2018, **48**(5): 790 - 800. DOI: 10.1109/TSMC.2016.2616347.

[11] Deng G L, Zhang Z W, Jiang T H, et al. Total flow time minimization in no-wait job shop using a hybrid dis-

crete group search optimizer[J]. *Applied Soft Computing*, 2019, **81**: 105480. DOI: 10.1016/j.asoc.2019.05.007.

[12] Sang Y W, Tan J P. Many-objective flexible job shop scheduling problem with green consideration[J]. *Energies*, 2022, **15**(5): 1 - 17. DOI: 10.3390/EN15051884.

[13] Gong G L, Deng Q W, Gong X R, et al. A new double flexible job-shop scheduling problem integrating processing time, green production, and human factor indicators [J]. *Journal of Cleaner Production*, 2018, **174**: 560 - 576. DOI: 10.1016/j.jclepro.2017.10.188.

[14] Ic Y T, Saraloğlu Güler E, Cabbaroğlu C, et al. Optimisation of cutting parameters for minimizing carbon emission and maximising cutting quality in turning process [J]. *International Journal of Production Research*, 2018, **56**(11): 4035 - 4055. DOI: 10.1080/00207543.2018.1442949.

[15] Li Y B, Huang W X, Wu R, et al. An improved artificial bee colony algorithm for solving multi-objective low-carbon flexible job shop scheduling problem[J]. *Applied Soft Computing*, 2020, **95**: 106544. DOI: 10.1016/j.asoc.2020.106544.

[16] Zhang M Y, Yan J H, Zhang Y L, et al. Optimization for energy-efficient flexible flow shop scheduling under time of use electricity tariffs[J]. *Procedia CIRP*, 2019, **80**: 251 - 256. DOI: 10.1016/j.procir.2019.01.062.

[17] Zhang Y F, Wang J, Liu Y. Game theory based real-time multi-objective flexible job shop scheduling considering environmental impact[J]. *Journal of Cleaner Production*, 2017, **167**: 665 - 679. DOI: 10.1016/j.jclepro.2017.08.068.

[18] Wang R B, Xu H Y, Guo J. Adaptive non-dominated sorting genetic algorithm [J]. *Control and Decision*, 2018, **33**(12): 2191 - 2196. DOI: 10.13195/j.kzyjc.2017.1032. (in Chinese)

[19] Ju L Y, Yang J J, Zhang J B, et al. Improved NSGA for multi-objective flexible job-shop scheduling problem[J]. *Computer Engineering and Applications*, 2019, **55**(13): 260 - 265, 270. DOI: 10.3778/j.issn.1002-8331.1809-0246. (in Chinese)

[20] Xu Y, Huang H S, Hu L. A hybrid immune genetic algorithm for job shop scheduling[J]. *Machinery Design and Manufacture*, 2020(9): 287 - 291. DOI: 10.19356/j.cnki.1001-3997.2020.09.067. (in Chinese)

面向绿色制造的轴承生产车间多目标调度优化

王彦森[1] 冯立杰[2,4] 王金凤[2,4] 刘 鹏[3,4] 赵华东[1]

([1] 郑州大学机械与动力工程学院, 郑州 450001)

([2] 上海海事大学中国(上海)自贸区供应链研究院, 上海 201306)

([3] 郑州大学管理学院, 郑州 450001)

([4] 河南省创新方法工程技术研究中心, 郑州 450001)

摘要:针对高性能轴承零部件的加工过程,以最大完工时间、机器加工碳排放量和磨削液使用量为目标函数,对轴承零部件加工的绿色车间调度问题进行研究.将轴承零部件的加工过程细化为启动、装夹、加工、卸夹、待机和关闭共6个流程,建立多目标绿色调度数学模型;提出了改进的多目标遗传算法进行求解,采用融合工序选择和机器选择的分段式编码方式,并在交叉、变异等步骤进行改进,提高算法收敛性;最后以某轴承公司的轴承零部件加工过程为例进行案例分析与对比试验,并通过大规模数据测试与分析.结果表明,所提模型可以得到更低的完工时间、碳排放量和磨削液使用量,从而验证了所提模型的科学性和有效性.

关键词:绿色车间调度;多目标优化;碳排放;轴承

中图分类号:TH278;TP30